ORIGINAL PAPER

Modification of composites of block copolymers–gold nanoparticles with enzymes and their characterization by electrochemical techniques

Rodrigo Del Río · Francisco Armijo ·
Ricardo Schrebler · Cesar Gutierrez · Andrea Amaro ·
Sonia R. Biaggio

Abstract In this work, the poly(styrene-vynil pyridine) block copolymer was used as a porous pattern to study the electrodeposition of gold inside the pores, as a new method to obtain gold nanoparticles. The porous pattern left by the copolymer film onto a conductive glass surface was characterized by atomic force microscopy (AFM), evidencing pores of 30 nm diameter. After the electrodeposition, 30 nm diameter gold nanoparticles were obtained and they were characterized by cyclic voltammetry (CV) and AFM, and then used to study the adsorption of glucose oxidase enzyme. The adsorption process of glucose oxidase on gold nanowires was investigated by CV and electrochemical impedance spectroscopy. The morphological and capacitance results indicate that the block copolymer–gold nanoparticle composite seems to be a good candidate to design biosensors and immunosensors.

Keywords Block copolymers · Gold nanowires · Copolymer–gold–enzyme composite

R. Del Río (✉) · F. Armijo · C. Gutierrez · A. Amaro
Facultad de Química, Pontificia Universidad Católica de Chile,
Avda Vicuña Mackenna 4860,
Macul, Santiago, Chile
e-mail: rdelrioq@uc.cl

R. Schrebler
Instituto de Química, Facultad de Ciencias Básicas
y Matemáticas, Pontificia Universidad Católica de Valparaíso,
Avda. Brasil 2850,
Valparaíso, Chile

S. R. Biaggio
Departamento de Química, Universidade Federal de São Carlos,
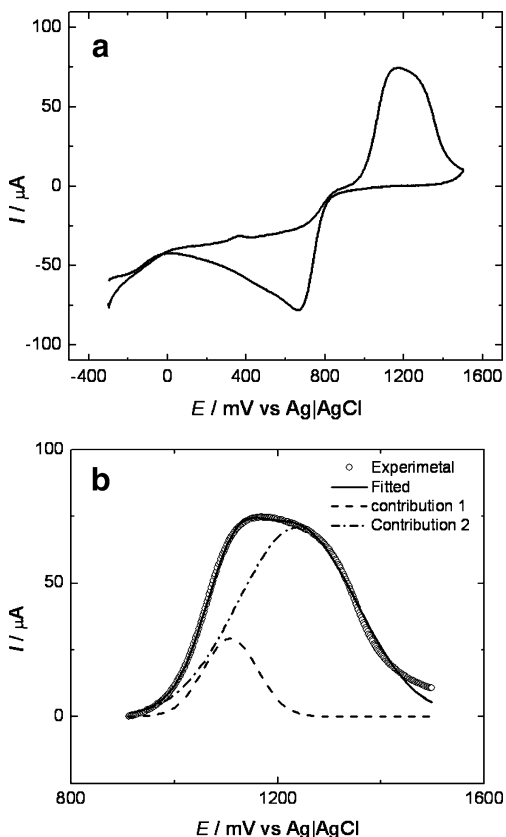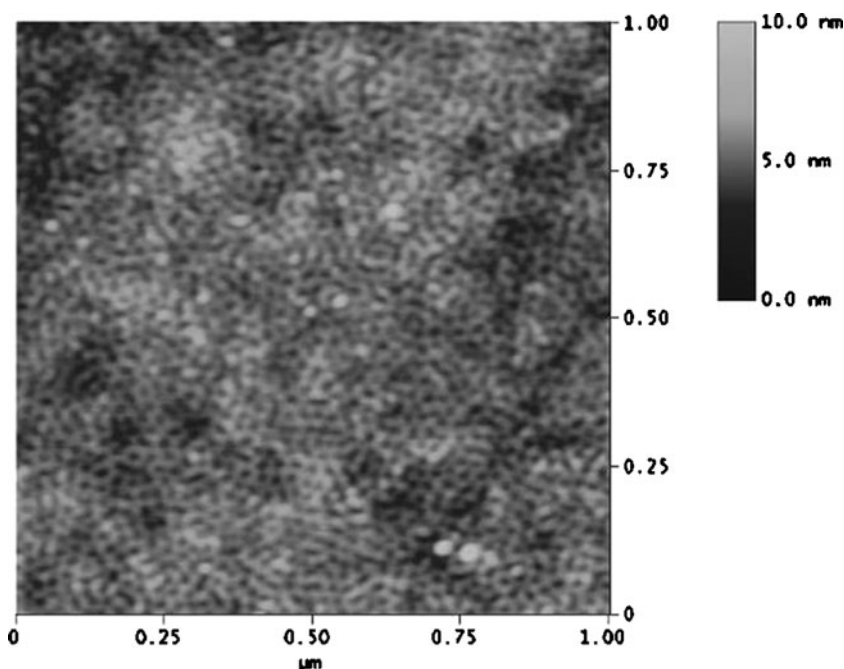C.P. 676, 13560-970 São Carlos, São Paulo, Brazil

Introduction

In the last years, synthesis of nanoparticles has received much attention [1]. Different metallic nanostructures have been obtained using alumina, polycarbonate and mesoporous silica membranes containing cylindrical pores [2–4]. These nanorods metallic structures might be used to design electrodes to sensing different species. Kumar et al. showed that gold nanoparticles with dehydrogenase enzyme catalyze the nicotinamide adenine dinucleotide oxidation, allowing to design an amperometric biosensor [5]. Tang et al. described a modified electrode composed by gold nanoparticles and immobilized hemoglobin, which was applied to the amperometric detection of hydrogen peroxide [6].

Other types of templates are block copolymers, which have been investigated due their ability to self assembled in different morphologies in nanoscopic range, such as, spherical, cylindrical, and lamellar depending on the volume of their blocks [7, 8]. These types of morphologies have received considerable attention as templates for the fabrication of high-density arrays of different elements that could be used in electronics devices [8–12]. These patterns could be assayed to obtain nanowires of different species [11]. The hydrophilic block is assembled forming the pores; sometimes a compound forming hydrogen bonding could be necessary to stimulate the porous pattern [12]. Park et al. demonstrated that highly oriented cylindrical microdomains can be achieved in thin films of poly(styrene-b-4-vinyl-pyridine) by spin coating the copolymer from a tetrahydro-furan/toluene solution [13].
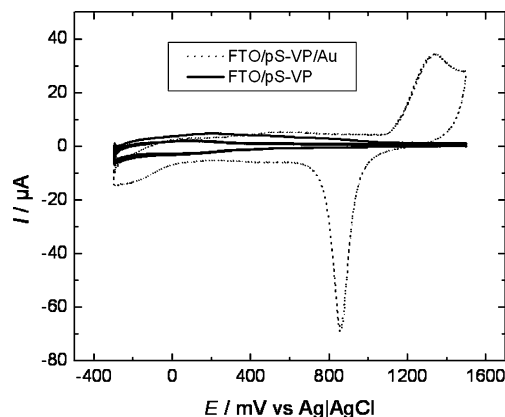
In general, all the electrodes composed by gold nano-particles, obtained using a template, were used as amper-ometric biosensors. In the field of biosensors, electrochemical impedance spectroscopy (EIS) is particu-

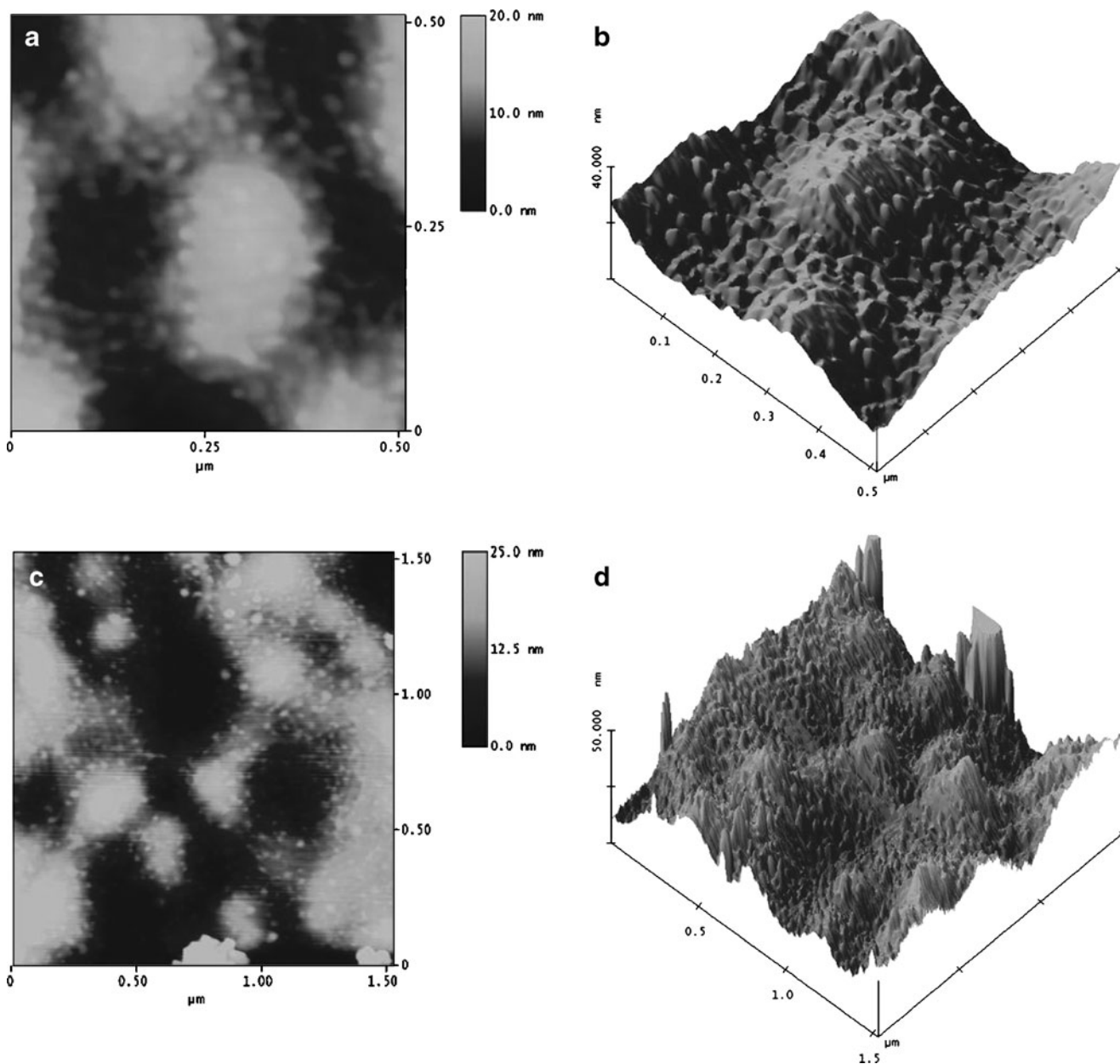**Fig. 1** AFM images of porous pattern of P(S-VP) film onto FTO glass

larly well-suited to the detection of binding events on the transducer surface. First examples of its use were reported at the end of the 1980s; however, the method has found increasing application in recent years due to advances made in instrumentation [14]. Besides the detection of biorecognition processes, it is a valuable tool for characterizing surface modifications, such as those that occur during the immobilization of biomolecules on the transducer. When taking measurements with such surface-modified sensing electrodes, redox-active compounds are commonly added to the solution, resulting in a well-defined charge transfer resistance R_{ct} [14]. If the redox-active compound is omitted or a blocking layer is applied to the electrode, a rather capacitive behavior will be observed in the impedance

Fig. 2 **a** Voltammetric profile at 0.1 Vs^{-1} of p(S-VP) film in 0.5 M H$_2$SO$_4$+10 mM AuCl$_4^-$. **b** Deconvolution of the anodic peak

Fig. 3 Voltammetric profile of gold nanoparticles in 0.5 M H$_2$SO$_4$ at 0.1 Vs^{-1}

Fig. 4 AFM images of gold nanoparticles obtained in a p(S-VP) pattern onto FTO electrodes

spectrum (since R_{ct} will become extremely large). Thus, a binding event at the electrode can be detected by following the change in R_{ct} in the first case or the change in the capacitance in the second case [14].

As an example, Wang et al. showed that fluorescein attached to gold nanoparticles changes the interfacial capacitance and the electrochemical impedance, when a gold electrode was exposed to "goat anti-fluorescein" [15]. Single frequency impedance measurements, performed at low frequencies, were found to be sensitive for R_{ct} changes, and the $K_4Fe(CN)_6$ used as electrolyte could induce the proteine denaturation.

In this work, gold nanoparticles were obtained by a new method of electrodeposition on a block copolymer tem-

plate. These nanoparticles were assayed as a substrate to study the adsorption of glucose oxidase [10–12], and cyclic voltammetry and electrochemical impedance spectroscopy were used to characterize the composite electrode [16, 17].

Experimental

The copolymer solution was obtained by dissolving 0.0107 g of 2-(4-hydroxybenzeneazo) benzoic acid (from Aldrich) and 0.0493 g of poly(styrene-*block*-(4-vinylpyridine)) copolymer—average molar masses (M_n) of 35,500 g/mol (PS), 3,680 g/mol, M_w/M_n=1.06 Polymer
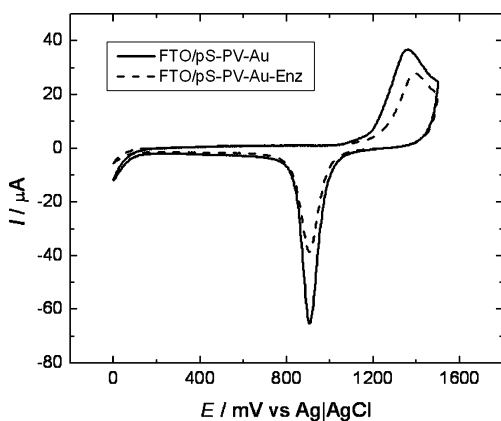
Fig. 5 Voltammetric profile of gold nanoparticles in 0.5 M H$_2$SO$_4$ at 0.1 Vs^{-1}, before (*continuous line*) and after (*dashed line*) the adsorption of glucose oxidase

Source, Inc.—in 2 mL of 2,4 dioxane. A 20 μL of this solution was casted (by spin coating) on a conductive glass (fluor-doped tin oxide, FTO from SOLEMS, France) at 1,500 rpm during 1 min. The resulting polymeric film was exposed to dioxane vapor during 24 h and used as working electrode for the electrodeposition of gold by applying a fix potential of 0.2 V during 20 min in a 20 mM AuCl$_4$$^-$ (obtained by dissolution of solid gold in aqua regia)/0.5 M H$_2$SO$_4$ (MERCK) aqueous electrolyte.

The electrochemical characterization of the composite electrode was performed by cyclic voltammetry in a 0.5 M H$_2$SO$_4$ electrolyte between −0.30 and 1.50 V (limits potentials to avoid of the hydrogen and water discharge interference), using a three-electrode electrochemical cell: the polymer–gold composite as the working electrode, a silver/sliver chloride electrode (Ag/ACl) as the reference, and a Pt foil as counter electrode. The electrochemical impedance spectroscopy was done in the same electrolyte, at

open circuit potential (E=0.100 V vs. SCE), in a frequency range of 10 mHz to 100 kHz and ac perturbation of 10 mV (rms), by means of a potentiostat CH 604 c (CH instruments) and an Ecochemie PGSTAT30 system. All solutions were kept at room temperature (approximately 23 °C).

The atomic force microscopy (AFM) images was performed in a Nanoscope IIIa (Digital Instruments) in tapping mode.

The enzyme adsorption on gold was performed from a 4.0 UE/mL glucose oxidase (ALDRICH) aqueous solution. A 20 μL of this solution was dipped on the composite surface for 20 min and then washed away with distilled water.
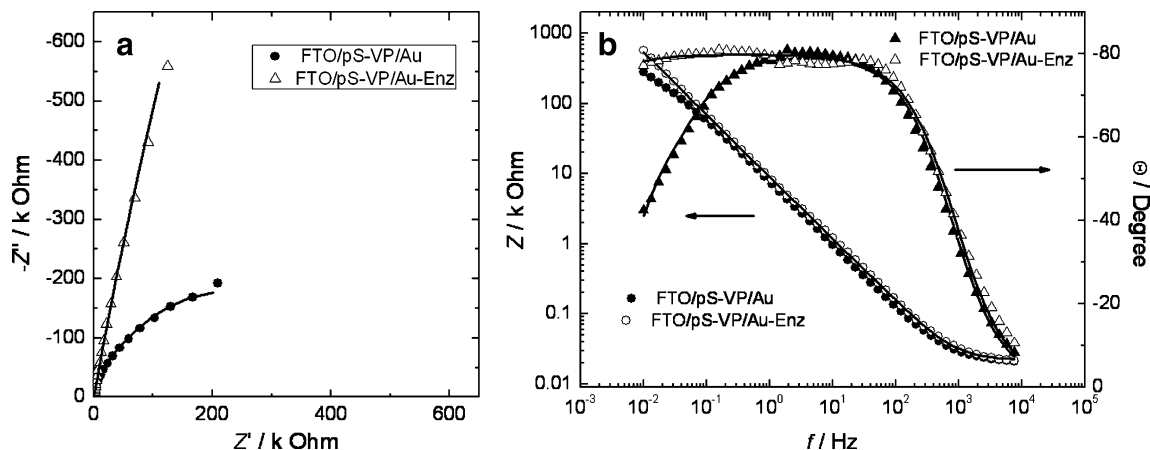
Results and discussion

Polymeric film and gold formation

Figure 1 shows the AFM images of the polymeric film deposited onto the substrate. These images show a well-ordered porous pattern on a homogeneous smooth film; the pores are of 30 nm diameter and homogeneously distributed. From these AFM images and considering the pores density on the image (400 pores μm^{-2}), it was possible to calculate the exposed area, which is about 25% of the surface geometric area. This parameter will be used to evaluate the full-filling of the pores by the gold electrodeposition.
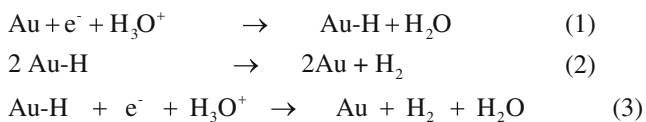
In order to obtain gold nanoparticles, the first condition to consider is the porous pattern used to modify the substrate electrode. The block copolymer forms porous films, and it is already reported that poly(styrene-b-vynil pyridine) was used to synthesize cobalt nanowires [12].

The polymeric film was used as working electrode to obtain electrodeposited gold according to the surface pattern defined above. Figure 2 shows the voltammetric response of the as-formed polymer–gold composite: a wide anodic peak

Fig. 6 a Nyquist diagram of gold nanoparticles in 0.5 M H$_2$SO$_4$ at open circuit potential, before (*solid circle*) and after (*open triangle*) the adsorption of glucose oxidase. **b** Bode diagram of gold nano-

particles in 0.5 M H$_2$SO$_4$ at open circuit potential, before (*solid triangle*) and after (*open triangle*) the adsorption of glucose oxidase

$$Au + e^- + H_3O^+ \quad \rightarrow \quad Au\text{-}H + H_2O \qquad (1)$$

$$2\,Au\text{-}H \quad \rightarrow \quad 2Au + H_2 \qquad (2)$$

$$Au\text{-}H + e^- + H_3O^+ \rightarrow \quad Au + H_2 + H_2O \qquad (3)$$

Scheme 1 Hydrogen evolution reaction mechanism [19]

is observed, which can be deconvoluted in two anodic peaks attributed to the gold growth in two different sites, inside the pores and outside the pores, the first anodic peak at 0.11 V correspond to the gold deposited outside the pores, comparing with the cyclic voltammetry (CV) profile of a bulk gold electrode in the same electrolyte (data not shown). The second peak corresponds to the gold deposited inside the pores. To avoid that the nanoparticle were deposited outside the pores, the potentiodynamic procedure was changed by a potentiostatic one and the cell configuration was changed and a more homogeneous deposit was obtained. This was done by placing a large area Pt plate parallel to the working electrode, and the results are analyzed below.
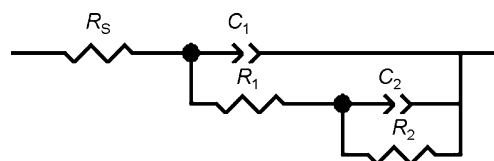
Electrochemical characterization

The gold electrodeposition conditions were optimized, and then the electrode was again characterized by CV. Figure 3 shows that only one well-defined anodic (and its corresponding cathodic) peak represents the gold voltammteric profile. From the electrical charge of the reduction peak (97 μC), a real electroactive area could be estimated, corresponding to 0.22 cm^2 of gold surface. Since the geometric area was about 1 cm^2, the eletrodeposited gold has 22% of the composite geometric area, which is consistent with the results obtained by AFM images.

The gold nanoparticles obtained were also characterized by AFM. In Fig. 4 it is possible to observe that the originals pores are missing and instead that the head of the nanoparticles with a diameter of 30 nm are observed, indicating that the gold fully filled the polymer pores. From the electrical charge calculated from Fig. 3, the active area of the gold electrodeposited corresponds to the area of the pores.

Enzyme adsorption

The gold nanoparticles or nanowires obtained by the pattern left by the copolymers were used to adsorb glucose oxidase. For this purpose, a glucose oxidase solution was dipped onto the electrode surface and the CV profiles were recorded before and after the adsorption process. Figure 5 shows these voltammetric profiles; the lowering of 30% of the total electrical charge observed after the dipping process indicates that the enzyme was adsorbed. Since the sharp-defined cathodic peak can be attributed to the reduction of a gold oxide monolayer formed at the considered potentials [18], one may conclude that the enzyme adsorption

Fig. 7 Equivalent circuit used to simulate the data of Fig. 6

provoked the partial blocking of the gold sites which would undergo oxidation.

Impedance characterization

Electrochemical impedance spectra were recorded for the composite electrode before and after the enzyme adsorption process. Figure 6a shows Nyquist diagrams for the enzyme modified and unmodified electrodes. Both electrodes showed a capacitive response and at any frequency, the total impedance (Z_T) was lower for unmodified electrode than enzyme modified electrode. The measurements were performed at the open circuit potential (approximately 0.1 V for both electrodes), in the potential range where the hydrogen evolution reaction takes place, as can be inferred from the voltammetric profile of Figure 3.

In order to simulate the electrochemical impedance data, a non-linear fit procedure was used considering the following expression for the total impedance:

$$Z_T = R_\infty + Z_{TF}$$

$$Z_{TF} = \left[\frac{1}{\left(R_1 \frac{1}{R_1^2} + \omega^2 C_1^2 \right)^{-1} + R_2 + i\omega C_1 \frac{1}{R_1^2} + \omega^{-2} C_1^{-2}} + (i\omega C_2)\alpha \right]^{-1}$$

where $\omega = 2\pi f$ and R_∞ denotes the ohmic resistance of the system. Z_{TF} is the transfer function of the system that contains the following elements: R_1 is the charge transfer resistance for the first electron transfer of the hydrogen evolution (see Eq. 1 in Scheme 1); C_1 is the capacitance due to the existence of hydrogen ad-atoms formed in this pathway (Eq. 2 in Scheme 1); R_2 is the charge transfer

Table 1 Calculated impedance parameters (defined in Fig. 7) for the copolymer–gold composites before and after the glucose oxidase enzyme adsorption

	FTO/pS-VP/Au	FTO/pS-VP/Au-Enz
R_S/Ohm	21.3	21.9
C_2/F	2.7 10^{-5}	2.0 10^{-5}
α	0.90	0.90
R_1/Ohm	2.8 10^5	1.8 10^7
C_1/F	6.2 10^{-5}	2.0 10^{-5}
α	1	1
R_2/Ohm	1.4 10^5	1.8 10^4

resistance associated to step (3); and C_2 is the double layer capacitance.

$$Au + e^- + H_3O^+ \rightarrow Au - H + H_2O \qquad (1)$$

$$2Au - H \rightarrow 2Au + H_2 \qquad (2)$$

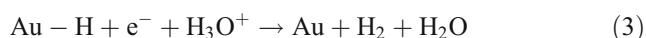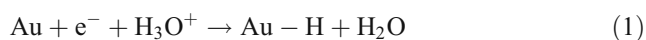$$Au - H + e^- + H_3O^+ \rightarrow Au + H_2 + H_2O \qquad (3)$$

Figure 6b shows experimental and simulated Bode diagrams for both composite electrodes. The equivalent circuit representing the total impedance (Z_T) is shown in Fig. 7, and was used to calculate the impedance parameters. The values of different contributions to the total impedance are presented in Table 1, where a good agreement between the experimental and simulated data can be observed. For both electrodes, R_1 values are higher than R_2 values, indicating that the water reduction process is controlled by the first charge transfer process, i.e., by the hydrogen ad-atoms formation. When the enzyme is present the values of R_1 increased, indicating that the rate of the pathway (1) is hindered and, consequently, a lower coverage for hydrogen ad-atoms is achieved. In general, the capacitance values decreased in a 30% rate in the presence of the enzyme. Considering that the electrode capacitance is proportional to the electroactive area, the impedance findings are consistent with the voltammetric results presented hereinbefore. This means that, in addition to other useful parameters like the electrolyte resistance and the charge transfer resistances, the impedance results can provide informations on the electrode area covered by the enzyme.

Conclusions

The poly(styrene-vynil pyridine) block copolymer was a good matrix to obtain gold nanoparticles electrodeposited in its pores. These gold nanoparticles of 30 nm diameter were found to be a good substrate to compose a gold-glucose oxidase electrode. The impedance data allowed to estimate the capacitance and, therefore, the electroactive area of the gold surface; the estimation of the electroactive area was confirmed by the voltammetric results. These findings basically indicate two things: (1) the obtained polymer–gold composite may be used as a biosensor based in gold nanoparticles; (2) the EIS results of charge transfer resistances and capacitances can be used as reliable parameters to evaluate the adsorption process.

References

1. Welch CM, Compton RG (2006) Anal Bioanal Chem 384:601–619
2. Martin CR (1994) Science 266:1961–1966
3. Huber CA, Huber TE, Sadoqui M, Lubin JA, Manalis S, Pratter CB (1994) Science 263:800–802
4. Fullam S, Cottell D, Rensmo H, Fitzmaurice D (2000) Adv Mater 12:1430–1432
5. Jena BK, Retna RC (2006) Anal Chem 78:6332–6339
6. Tang M, Chen S, Yuan R, Chai Y, Gao, Xie Y (2008) Anal Science 24:487–491
7. Park H, Harrison C, Chaikin PM, Register RA, Adamson DH (1997) Science 276:1401–1404
8. Thum-Albrecht T, Schotter J, Kastle CA, Emley N, Shibuachi T, Krusin-Elbaum L, Guarani K, Black CT, Touminen M, Russell TP (2000) Science 290:2126–2129
9. Fan HJ, Werner P, Zacharias M (2006) Small 2:700–717
10. Hamley AIW (2003) Nanotechnology 14:R39–R54
11. Lin Y, Böker A, He J, Sill K, Xiang H, Abetz C, Li X, Wang J, Emrick T, Luna S, Wang Q, Balazs A, Rusell TP (2005) Nature 434:55–59
12. Siderenko I, Tokarev S, Minko M, Stamm M (2003) J Am Chem Soc 125:12211–12216
13. Park S, Wang J, Kim B, Chen W, Russell TP (2007) Macromolecules 40:9059–9063
14. Listad F, Schafer D (2008) Anal Bioanal Chem 391:1555–1567
15. Wang J, Profitt JA, Pugia MJ, Suni II (2006) Anal Chem 78:1769–1773
16. Xiao Y, Patolsky F, Katz E, Hainfeld JF, Willner I (2003) Science 299:1877–1881
17. Yañez-Sedeño P, Pingarrón JM (2005) Anal Bioanal Chem 382:884–886
18. Yu JJ, Lu S, Li JW, Zhao FQ, Zeng BZ (2007) J Solid State Electrochem 11:1211–1219
19. Córdova R, Gómez H, Schrebler R, Cury P, Orellana M, Grez P, Leinen D, Ramos-Barrado JR, Del Rio R (2002) Langmuir 18:8647–8654